An assessment of the correlation between robust CT-derived ventilation and pulmonary function test in a cohort with no respiratory symptoms

Nair, Girish B.; Galban, Craig J.; Al-Katib, Sayf; Podolsky, Robert; van den Berge, Maarten; Stevens, Craig; Castillo, Edward

Published in:
British journal of radiology

DOI:
10.1259/bjr.20201218

Publication date:
2021

BJR

https://doi.org/10.1259/bjr.20201218

Received: 09 October 2020 | Revised: 30 November 2020 | Accepted: 01 December 2020

Cite this article as:
Nair GB, Galban CJ, Al-Katib S, Podolsky R, van den Berge M, Stevens C, et al. An assessment of the correlation between robust CT-derived ventilation and pulmonary function test in a cohort with no respiratory symptoms. *Br J Radiol* 2020; **94**: 20201218.

SHORT COMMUNICATION

An assessment of the correlation between robust CT-derived ventilation and pulmonary function test in a cohort with no respiratory symptoms

[1]GIRISH B NAIR, [2]CRAIG J GALBAN, [3]SAYF AL-KATIB, [4]ROBERT PODOLSKY, [5]MAARTEN VAN DEN BERGE, [6]CRAIG STEVENS and [6,7]EDWARD CASTILLO

[1]Division of Pulmonary and Critical Care, Beaumont Health, OUWB School of Medicine, Auburn Hills, MI, USA
[2]Department of Radiology, University of Michigan, Ann Arbor, MI, USA
[3]Department of Radiology and Molecular Imaging, Beaumont Health, OUWB School of Medicine, Auburn Hills, MI, USA
[4]Division of Informatics & Biostatistics, Beaumont Research Institute, Beaumont Health, Beaumont, TX, USA
[5]Department of Pulmonary Disease, University Medical Center Groningen, Groningen, The Netherlands
[6]Department of Radiation Oncology, Beaumont Health, OUWB School of Medicine, Auburn Hills, MI, USA
[7]Department of Computational and Applied Mathematics, Rice University, Houston, TX, USA

Address correspondence to: Dr Edward Castillo
E-mail: *Edward.Castillo@beaumont.edu*

Objective: To evaluate CT-ventilation imaging (CTVI) within a well-characterized, healthy cohort with no respiratory symptoms and examine the correlation between CTVI and concurrent pulmonary function test (PFT).
Methods: CT scans and PFTs from 77 Caucasian participants in the NORM dataset (clinicaltrials.gov NCT00848406) were analyzed. CTVI was generated using the robust Integrated Jacobian Formulation (IJF) method. IJF estimated total lung capacity (TLC) was computed from CTVI. Bias-adjusted Pearson's correlation between PFT and IJF-based TLC was computed.
Results: IJF- and PFT-measured TLC showed a good correlation for both males and females [males: 0.657, 95% CI (0.438–0.797); females: 0.667, 95% CI (0.416–0.817)]. When adjusting for age, height, smoking, and abnormal CT scan, correlation moderated [males: 0.432, 95% CI (0.129–0.655); females: 0.540, 95% CI (0.207–0.753)]. Visual inspection of CTVI revealed participants who had functional defects, despite the fact that all participant had normal high-resolution CT scan.
Conclusion: In this study, we demonstrate that IJF computed CTVI has good correlation with concurrent PFT in a well-validated patient cohort with no respiratory symptoms.
Advances in knowledge: IJF-computed CTVI's overall numerical robustness and consistency with PFT support its potential as a method for providing spatiotemporal assessment of high and low function areas on volumetric non-contrast CT scan.

INTRODUCTION

Conventional CT imaging of the thorax offers detailed information concerning the structural integrity of the lung parenchyma. While this information is valuable, a normal structural appearance does not guarantee that the underlying lung function is also normal. As such, direct visualization of lung function is a valuable compliment to convention CT that enables the identification of low functional regions with apparently normal parenchymal structure.

Automated methods for categorizing lung parenchyma based on imaging features and textures have demonstrated a good correlation with lung function parameters and pathological changes.[1–3] These techniques typically train a classification or machine learning model to identify and grade disease patterns according to training data acquired from expert radiologist consensus. However, consensus training lacks an ability to identify changes beyond the visually recognizable patterns, is mostly semi-quantitative, and does not provide information regarding quantitative lung function – such as ventilation and perfusion. Hence, the ability to recover functional information from standard inspiration and expiration CT (IE-CT) scans could be potentially useful for delineating and quantifying longitudinal parenchymal and airway-related changes.

CT-derived ventilation imaging (CTVI) is an image processing-based modality that recovers changes in local tissue volumes, induced by respiratory motion, from IE-CT scans. Since changes in air content are the primary driver for the volume changes observed during breathing, CTVI was developed and subsequently established as a surrogate

Figure 1. Areas of decreased ventilation in study participants with normal CT scan are denoted with bold arrows. Top Row: (a) An axial slice from the CT of a smoker appears normal, while the CTVI (b) shows an area of decreased ventilation in the right middle lobe. Bottom Row: (c) An axial CT slice from a non-smoker also appears normal, while the CTVI (d) shows an area of decreased function. CTVI, CT-derived ventilation imaging.

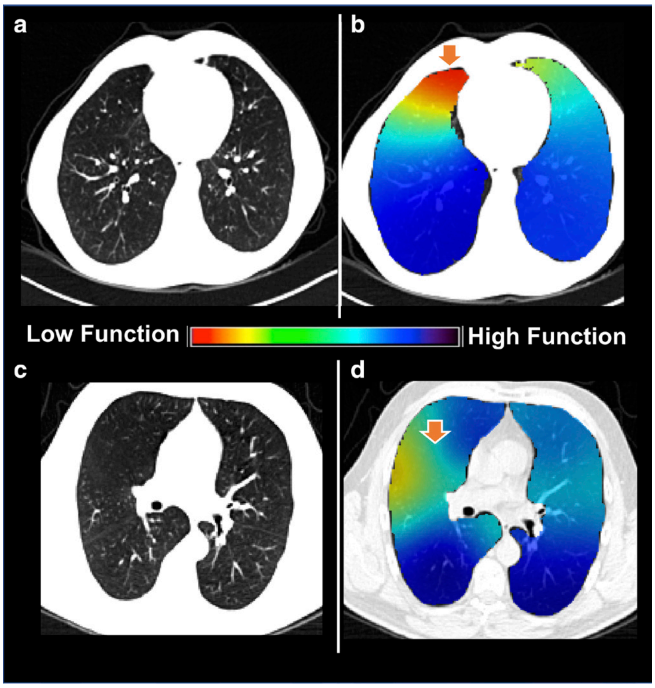

for ventilation imaging.[4] CTVI was originally developed for radiation oncology applications where dynamic free-breathing CT (4DCT) is acquired as standard-of-care.[4] However, issues related to low reproducibility[5,6] have hindered wide-spread clinical adoption of CTVI and limited the range of its potential applications to those that are generally qualitative in nature. For instance, CTVI has demonstrated effectiveness as the basis for radiotherapy functional avoidance planning in lung cancer.[7] A recently derived mathematical theory identified numerical instability as a key driver of the CTVI variability reported in the literature.[8] This allowed for the development of a new class of robust CTVI algorithms designed to address reproducibility issues.[9] In addition to improved robustness, one such algorithm, the Integrated Jacobian formulation (IJF) method, was recently shown to have a higher spatial correlation with single positron emission computed tomography (SPECT) ventilation than any other CTVI method previously reported in the literature.[10] Moreover, the increased physiological fidelity afforded by IJF has widened the scope of potential applications to include estimating lung compliance[11] and quantifying disease progression of idiopathic pulmonary fibrosis.[12]

The purpose of this cross-sectional study is to evaluate IJF computed CTVI among patients from a well-characterized, healthy cohort with no respiratory symptoms and examine the correlation between IJF-measured total lung capacity and concurrent pulmonary function test (PFT).

METHODS AND MATERIALS

Integrated Jacobian formulation images and TLC

The IJF method was applied to IE-CTs to recover the apparent voxel volume changes, induced by varying lung inspiratory levels, as a surrogate for pulmonary ventilation. The utilized software implementation of IJF follows the description in.[9,10] Briefly, like other CTVI methods, IJF requires three computational steps: (1) lung volume delineation (segmentation), (2) deformable image registration (DIR) for lung motion recovery, and (3) the IJF CTVI calculation. In contrast to other CTVI approaches that are based on numerically unstable single voxel measurements,[8] IJF estimates the Jacobian factor of the DIR transformation (*i.e.* volume change) from a series of spatially corresponding inhale/exhale subregions. The numerical uncertainty in the subregional volume change measurements is modeled with gaussian statistics, which allows for the uncertainty associated with the measurements to be both characterized and controlled. IJF computes CTVI by solving a linear least squares problem which defines individual voxel volume changes in terms of the series of robust subregional measurements.

DIR and the IJF calculation follow the implementation described in Castillo et al.[10] The required lung segmentation was computed automatically using a convolutional neural network (U-NET) implemented in MATLAB (release R2019a, The Mathworks Inc, Natick, MA) and manually inspected for quality assurance. The resulting IJF solution quantifies breathing-induced volume change for each lung voxel, thus providing a full volumetric image of ventilation (Figure 1). TLC can be computed directly from IJF CTVI by summing the intensity values of all voxels within the lung volume.

Images and patient data

CT scans from 77 Caucasian participants in the NORM data set (clinicaltrials.gov NCT00848406) were used for this study. All included patients were older than 18 years of age and had no respiratory symptoms or diseases. Participants were classified into smokers (n = 44) *vs* non-smokers (n = 33) (Table 1). All subjects had normal pulmonary function. Total lung capacity (TLC) is the volume of air retained within the lungs upon the maximum inhalation. Similar to findings in other studies,[13] mean TLC of both PFT and IJF significantly differed between males and females. As such, all subsequent analyses were done separately for males and females. Since lung function is correlated to age, sex, height, smoking status and ethnicity, we analyzed a uniform population of Caucasians and separately analyzed the covariates for males and females.

Statistical analysis

We examined the correlation between PFT and IJF-based TLC using bias-adjusted Pearson's correlation, and calculated 95% confidence intervals (CIs) using the Fisher z-transformation. We also examined partial correlations between PFT and IJF-based TLC, adjusting for age, height, smoking, and abnormal CT scan. Finally, we examined the association between IJF-based TLC and age and height using a linear model that included those variables along with covariates for smoking and abnormal CT scan noted by radiologist.

Table 1. Baseline characteristics between smokers and non-smokers

	Smokers (n = 44)	Non-smoker (n = 33)	Significance
Age in years	39	38	0.55
Height (cm)	177.0	174.9	0.25
Weight (Kg)	73.89	73.04	0.76
Female	25%	21%	0.65
Atopy history	12.5%	17.5%	0.06
Work exposure history	11.1%	13.6%	0.22
Forced vital capacity (L)	5.04	4.93	0.63
Total lung capacity (L)	6.93	6.78	0.60
IJF quantitative total ventilation (L)	5.80	5.70	0.73
Right lung IJF (L)	3.06	3.03	0.85
Left lung IJF (L)	2.73	2.65	0.62

IJF, Integrated Jacobian formulation.

RESULTS

The baseline characteristics showed no significant differences between the 44 smokers and 33 non-smokers (Table 1). Neither PFT- nor IJF-based TLC differed significantly between smokers and non-smokers, even when separately analyzed for males and females. Pearson correlation between TLC determined using IJF and PFT showed a moderate correlation for both males and females [males: 0.657, 95% CI (0.438–0.797); females: 0.667, 95% CI (0.416–0.817)]. These correlations were not as strong when adjusting for age, height, smoking, and abnormal CT scan [males: 0.432, 95% CI (0.129–0.655); females: 0.540, 95% CI (0.207–0.753)]. IJF-based TLC was significant only when correlated with height for both males (p = 0.0001) and females (p = 0.0040) when adjusting for age, smoking history and abnormal CT scan (Table 2). Regional analyses of IJF CTVI (Figure 1) showed several cases (23/77) showing low function with decreased ventilation score, although there was no visible corresponding radiographic abnormality on High resolution CT (HRCT) scan at full inflation (*i.e.* inspiration).

DISCUSSION

Lung function assessed by PFT is highly subjective and is heavily dependent on cooperation and efforts from patient and technician in performing the test correctly. The robust IJF CTVI method for quantifying lung function from volumetric CT scan evaluated in this study correlates well with traditional PFT-derived lung function. While our results show a good correlation between TLC derived from PFT and IJF, when analyzed separately between males and females, the correlation decreases. Sex differences in lung function is well characterized and our results further authenticate differences in lung function between males and females.[13] Subject's height was the major determinant for TLC obtained from IJF for both males and females. This is consistent with previous studies on factors affecting lung function.[14]

Table 2. Bias adjusted correlation between IJF-defined total lung capacity and correlates

	Estimated correlation	95% confidence limits		Significance
Males:				
Age	0.019	−0.001	0.039	0.0678
Height	0.108	0.057	0.160	0.0001
Non-smoker	0.122	−0.568	0.811	0.7230
Atopy	−0.148	−0.855	0.559	0.6745
Source	**Estimated correlation**	**95% confidence limits**		**Significance**
Females:				
Age	0.004	−0.019	0.027	0.734
Height	0.084	0.029	0.139	0.004
Non-smoker	0.032	−0.618	0.682	0.920
Atopy	0.124	−0.622	0.871	0.735

IJF, Integrated Jacobian formulation.
The four correlates (Age, Height, Smoking Status, Atopy) are examined in both males and females.

Our results are noteworthy for several reasons. First, IJF is a direct derivative of actual deformation within each lung voxel, which is numerically stable and reproducible. Hence, the volumes derived are much more substantive and reliable than most current methods using semi-quantitative lung texture analysis.[15] Secondly, the fact that IJF correlates well with TLC derived from PFT in both males and females, but is able to discriminate areas of lung which are not participating in ventilation is significant. These functional defects apparent on CTVI had no apparent changes visible on HRCT. Whether these defects eventually develop into lung abnormality is unknown from the current data. Thirdly, height was the significant predictor for IJF after adjusting for all other parameters, which corroborates and validates the IJF derived ventilation parametric as seen with PFT.[14]

Although the study was robust and had sufficient power to detect changes and correlations, it was limited by certain factors. This study was cross-sectional and neither the data nor imaging required to pursue regional ventilation changes longitudinally were available. Now that we have established a reproducible way of accurately quantifying lung function from IE-CT images, our immediate future work will compare the clinical accuracies of IJF-defined high- and low-ventilation regions with those determined from currently available quantitative imaging tools, as well as further investigate the relationship between CTVI-defined defects and the development of lung abnormalities.

CONCLUSION

The presented study demonstrates that total lung capacity derived from IJF correlates moderately well with TLC obtained from PFT. Taken together with CTVI's ability to spatially discriminate regions of low *vs* high lung function, these results are indicative of CTVI's potential to characterize lung function and identify disease presence.

REFERENCES

1. Jacob J, Bartholmai BJ, Rajagopalan S, van Moorsel CHM, van Es HW, van Beek FT, et al. Predicting outcomes in idiopathic pulmonary fibrosis using automated computed tomographic analysis. *Am J Respir Crit Care Med* 2018; **198**: 767–76. doi: https://doi.org/10.1164/rccm.201711-2174OC
2. Lee SM, Seo JB, Oh SY, Kim TH, Song JW, Lee SM, et al. Prediction of survival by texture-based automated quantitative assessment of regional disease patterns on CT in idiopathic pulmonary fibrosis. *Eur Radiol* 2018; **28**: 1293–300. doi: https://doi.org/10.1007/s00330-017-5028-0
3. Salisbury ML, Lynch DA. Toward early identification of clinically relevant interstitial lung disease. *Am J Respir Crit Care Med* 2017; **196**: 1368–9. doi: https://doi.org/10.1164/rccm.201706-1235ED
4. Vinogradskiy Y. Ct-Based ventilation imaging in radiation oncology. *BJR|Open* 2019; **1**: 20180035. doi: https://doi.org/10.1259/bjro.20180035
5. Yamamoto T, Kabus S, Klinder T, von Berg J, Lorenz C, Loo BW, et al. Four-Dimensional computed tomography pulmonary ventilation images vary with deformable image registration algorithms and metrics. *Med Phys* 2011; **38**: 1348–58. doi: https://doi.org/10.1118/1.3547719
6. Yamamoto T, Kabus S, von Berg J, Lorenz C, Chung MP, Hong JC, et al. Reproducibility of four-dimensional computed tomography-based lung ventilation imaging. *Acad Radiol* 2012; **19**: 1554–65. doi: https://doi.org/10.1016/j.acra.2012.07.006
7. Vinogradskiy Y, Rusthoven CG, Schubert L, Jones B, Faught A, Castillo R, et al. Interim analysis of a two-institution, prospective clinical trial of 4DCT-ventilation-based functional avoidance radiation therapy. *Int J Radiat Oncol Biol Phys* 2018; **102**: 1357–65. doi: https://doi.org/10.1016/j.ijrobp.2018.07.186
8. Castillo E, Castillo R, Vinogradskiy Y, Guerrero T. The numerical stability of transformation-based CT ventilation. *Int J Comput Assist Radiol Surg* 2017; **12**: 569–80. doi: https://doi.org/10.1007/s11548-016-1509-x
9. Castillo E, Castillo R, Vinogradskiy Y, Dougherty M, Solis D, Myziuk N, et al. Robust CT ventilation from the integral formulation of the Jacobian. *Med Phys* 2019; **46**: 2115–25. doi: https://doi.org/10.1002/mp.13453
10. Castillo E, Castillo R, Vinogradskiy Y, Nair G, Grills I, Guerrero T, et al. Technical note: on the spatial correlation between robust CT-ventilation methods and SPECT ventilation. *Med Phys* 2020; **47**: 5731–8. doi: https://doi.org/10.1002/mp.14511
11. Nair GB, Castillo E. Longitudinal lung compliance imaging in idiopathic pulmonary fibrosis. *Radiology* 2019; **293**: 272. doi: https://doi.org/10.1148/radiol.2019191115
12. Nair GB, Al-Katib S, Castillo E. Pulmonary blood mass and quantitative lung function imaging in idiopathic pulmonary fibrosis. *Radiology* 2020; **2**: e200003. doi: https://doi.org/10.1148/ryct.2020200003
13. LoMauro A, Aliverti A. Sex differences in respiratory function. *Breathe* 2018; **14**: 131–40. doi: https://doi.org/10.1183/20734735.000318
14. Luzak A, Fuertes E, Flexeder C, Standl M, von Berg A, Berdel D, et al. Which early life events or current environmental and lifestyle factors influence lung function in adolescents? - results from the GINIplus & LISAplus studies. *Respir Res* 2017; **18**: 138. doi: https://doi.org/10.1186/s12931-017-0619-5
15. Chen A, Karwoski RA, Gierada DS, Bartholmai BJ, Koo CW. Quantitative CT analysis of diffuse lung disease. *Radiographics* 2020; **40**: 28–43. doi: https://doi.org/10.1148/rg.2020190099